energies

MDPI

Article

Study on the Evaluation Index System and Evaluation Method of Voltage Stability of Distribution Network with High DG Penetration

Jingjing Tu *, Zhongdong Yin and Yonghai Xu

School of Electrical & Electronic Engineering, North China Electric Power University, Beijing 102206, China; yzd@ncepu.edu.cn (Z.Y.); yonghaixu@263.net (Y.X.)

* Correspondence: shell2005@126.com; Tel.: +86-010-6026-0765

Received: 30 November 2017; Accepted: 27 December 2017; Published: 1 January 2018

Abstract: With the development of new energy technologies, distributed generation (DG) plays a growing role in power distribution networks. Although it solves the power supply problem in some areas, it also poses a challenge to the traditional power grid. To help with this problem, we establish a static voltage stability analysis model for high penetration DG, taking into account its large capacity, and the high fluctuations of its output. Based on the theoretical analysis and the mathematical derivation, we propose an improved voltage stability evaluation index (IVSE) accounting for DG. Finally, using the typical circuit of the IEEE 33 & 69 node system, we simulate high penetration DG access in different locations and capacities. In the simulations, the traditional power flow equation is modified by a continuous parametric equation accounting for DG. Based on consideration of the system transmission power limit, voltage stability margin and system loss, the value of IVSE is demonstrated, in comparison with the traditional index. Thus, we verify that the IVSE index is easy to understand, simple to calculate, and highly versatile.

Keywords: DG; IVSE; centralized; decentralized; different capacity; voltage stability margin; PV curve

1. Introduction

In recent years, the field of distributed generation (DG) for power generation has developed rapidly, helping to reduce the demand for traditional fossil-based energy sources, producing less polluting emissions, and protecting the environment. At the end of 2015, China's cumulative installed capacity of wind power had reached 128.3 GW, while its solar power installed capacity reached 43.18 GW. Looking at the ratio between the new energy installed capacity and the maximum load (that is, new energy penetration), China is at 22%, a moderate level [1], higher than the United States (10%), but lower than Denmark (93%), Spain (78%), and Portugal (63%). As the influence of wind and photovoltaic power increases, it interferes more with the power grid, seriously affecting the stability and reliability of system voltage.

More and more DGs [2] are being introduced into the distribution network. Compared with conventional units, these DGs have some special features: their equivalent moment of inertia is small, the primary frequency modulation capacity is lacking, and their voltage regulation capacity is limited. If new energy units replace a large number of conventional power supplies, it will reduce the anti-disturbance capability of the power grid; in particular, high power shock conditions can induce voltage problems in the whole network. Meanwhile, the distribution network becomes one with a low voltage level, variable load, and poor anti-interference ability. Beyond a certain amount of DG access, the traditional distribution network changes into a complex net with multi-point power supplies [3,4], which above all will have a great impact on the voltage stability of the distribution network. Therefore,

determining the weakness of the network quickly and easily, and finding the best access location of DG while giving the optimal access capacity, is a popular topic in current research.

In [5], the impact of the load recovery and instability characteristics on the voltage stability of the system are introduced, a load model that is suitable for voltage stability analysis is established, and the voltage stability control measures are given. In [6], based on the analysis of the cause of system transient voltage instability, the model of differential algebraic equation is presented, and the energy function is used to judge the transient voltage stability of the system. Aiming at the problem of voltage and reactive power caused by large-scale wind farms connected to the power grid, Reference [7] proposes a reactive power control strategy for wind farms to improve the voltage stability of the access area. Reference [8] studies the influence of photovoltaic access to the grid on voltage stability, and establishes a unified circuit model of a photovoltaic grid connected system based on the concept of generalized load. Reference [9] presents the comprehensive index of safety of distribution network by calculating the stability of the wind farm power circle, the safety of power grid structure, and the reliability of user electricity. Reference [10] deduces the voltage stability criterion by power flow calculation, and gives out the conditions for the use of the criterion according to the characteristics of load changes. Reference [11], against the system load fluctuation limit, from the voltage, load node types, and network capacity, presents a risk evaluation index, to determine the weak areas of the system. In [12], the paper presents a decision-making algorithm that has been developed for the optimum size and placement of DGs in distribution networks, based on the improvement of voltage profile and the reduction of the network's total power losses. The proposed algorithm has been tested on the IEEE 33-bus radial distribution system. The worldwide continuous integration of DGs in electric power systems is a result of the privatization of electricity markets, environment protection from emissions, and technological progression. The unadvised and uncontrolled installation of DGs in the distribution network during the past two decades brought in serious problems and challenges to the distribution networks. In [13], the impact of DGs on the distribution networks' voltage profile and energy losses is introduced in detail.

It can be seen from the above that existing studies mainly study the issue from one perspective, for example, the voltage stability. For specific problems, existing studies tend to build their own load models, then use conventional power flow calculations to do an analysis, and put forward various voltage stability evaluation indexes of original design, and they mainly do voltage stability and reactive power control strategy studies. These kinds of indexes have a more complex computational form, and the corresponding constraints are of poor generality and require long calculation times.

In this paper, based on high penetration DG access with different positions and capacities, under the premise of varied voltage profile, load growth mode and active loss, an improved voltage stability evaluation index (IVSE) is proposed. The theory of this index is simple to calculate and easy to understand, and it is flexible to modify according to demand, so as to reflect the impact of DG access on the distribution network. By establishing a static voltage stability analysis model that accounts for DG operating characteristics [14], then modifying the conventional power flow calculation equation and using IEEE 33 & 69 to do simulations, this IVSE index is compared with the traditional VSE index, so as to show the correctness and validity of the proposed index. The proposed IVSE index can provide an efficient reference to engineers, electric utilities, and researchers and so on, on handling the optimization problems concerning high penetration of DGs in distribution networks.

2. Voltage Stability Evaluation Index (VSE)

2.1. Traditional VSE

An important role of the voltage stability evaluation index (VSE) is to determine the weak lines or buses in a network [15,16]. During calculation, the extreme value of the index is given under different constraints, and the closer the VSE is to this extreme, the weaker the line or bus corresponding to the index [17,18]. Therefore, this index is usually used for DG optimization of location and capacity.

In general, the application of the VSE is divided into two steps. First, the weakest point of the network is determined by VSE based on the line or bus. Then, the voltage stability margin of each node is calculated according to the global index value, to perform subsequent accurate calculation and analysis [19,20].

An N-node distribution network, according to the Thevenin's equivalent theorem, is equivalent to the single-line circuit shown in Figure 1 [21]. The quadratic equation for the node voltage must be solved to get the VSE.

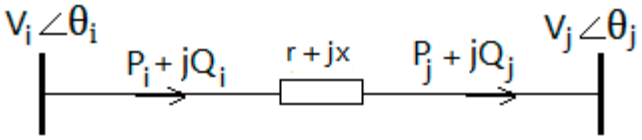

Figure 1. A simple radial system network.

In Figure 1, node i is the input node, whose voltage is $U_i \angle \theta_i$, and whose input power is $P_i + jQ_i$; node j is the output node, whose voltage is $U_j \angle \theta_j$, and whose input power is $P_j + jQ_j$; the line impedance is $r + j_x$, ignoring the admittance. The following relations hold:

$$P_j + jQ_j = S_j = \dot{U}_j \dot{I}_i^* \tag{1}$$

$$\dot{I}_i = \frac{U_i \angle \theta_i - U_j \angle \theta_j}{r + jx} \tag{2}$$

Substituting Equation (2) into Equation (1), and identifying the real and imaginary parts respectively, yields:

$$P_j r + Q_j x = U_i U_j \cos\theta - U_j^2 \tag{3}$$

$$P_j x - Q_j r = U_i U_j \sin\theta \tag{4}$$

If the voltage phase angle of each node in the distribution network only differs slightly, so that $\theta_i \approx \theta_j$, then one obtains the simplified quadratic equation for the voltage:

$$\frac{r}{x} U_j^2 - \frac{r}{x} U_i U_j + \left(\frac{r^2}{x} - x \right) P_j + 2Q_j r = 0 \tag{5}$$

Inspecting the quadratic equation's discriminant, one defines:

$$VSE = \frac{4Q_j (r^2 + x^2)}{x U_i^2} \leq 1 \tag{6}$$

When VSE is closer to 1, the line is closer to the critical operating state, while when the VSE value is smaller, the voltage stability is better. The node with the largest VSE value is the weakest node in the system. The difference between VSE and 1 determines the voltage stability margin of the node and the system.

As reflected in the PV curve [22,23] (see Figure 2), when the operating point is located on the curve's upper portion, the system voltage remains stable. When the load demand increases, the node voltage drops, until the nose point of the PV curve, where the voltage stability limit is reached. The distance between the running point and the nose of the PV curve represents the size of the node voltage stability margin.

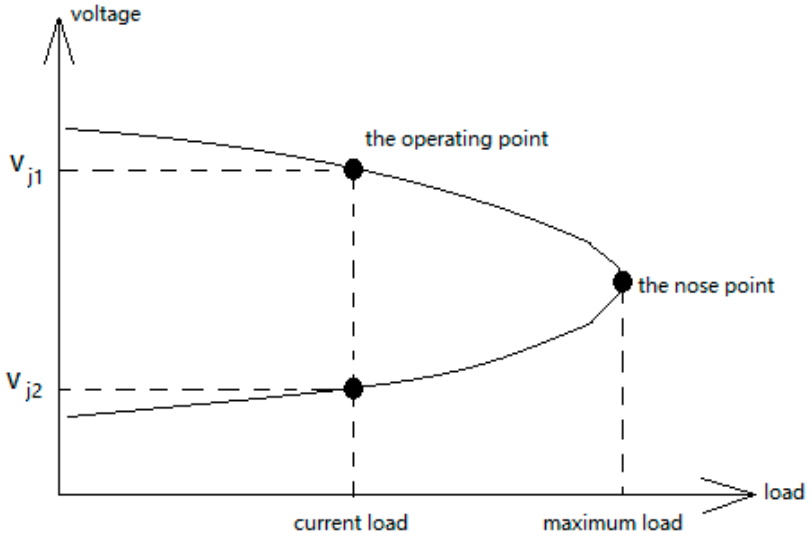

Figure 2. PV curve of the system from Figure 1.

2.2. Static Voltage Stability Analysis Model with High Penetration DG

In the existing literature, DG is usually equivalent to an impedance with a current source, with access into the load as a kind of negative power. One then performs a conventional power flow calculation, producing the system power and voltage distribution. In this paper, we use the method proposed in [14] to establish the static voltage stability analysis model considering DG, perform the Thevenin's equivalent theory to establish a continuous parameter equation, and use this equation to correct the conventional power flow calculation, thus obtaining the new distribution of the system power and voltage. Then, substituting the relevant parameters into the formula for the voltage stability evaluation index yields the improved voltage stability evaluation index (IVSE) and corresponding stability margin of each node in the system, taking into account the DG effect.

From Figures 3 and 4, before DG access,

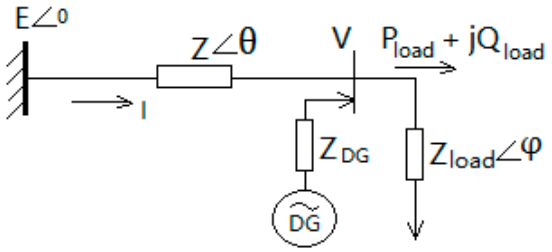

Figure 3. Distribution diagram with DG.

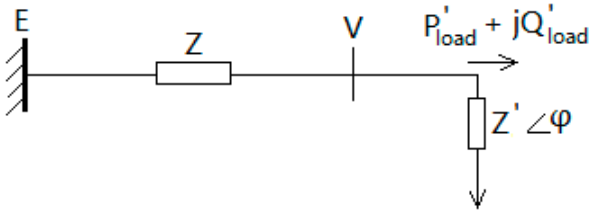

Figure 4. Distribution equivalent diagram with DG.

$$I = \frac{E}{\sqrt{(Z\cos\theta + Z_{load}\cos\varphi)^2 + (Z\sin\theta + Z_{load}\sin\varphi)^2}} \tag{7}$$

Equation (7) can be simplified as:

$$I = \frac{1}{\sqrt{F}}\frac{E}{Z}, \tag{8}$$

where

$$F = 1 + \left(\frac{Z_{load}}{Z}\right)^2 + 2\left(\frac{Z_{load}}{Z}\right)\cos(\theta - \varphi) \tag{9}$$

Thus:

$$U = Z_{load}I = \frac{1}{\sqrt{F}}\frac{Z_{load}}{Z}E \tag{10}$$

Substituting Equations (8)–(10), and simplifying:

$$P = UI\cos\varphi = \frac{Z_{load}}{F}\left(\frac{E}{Z}\right)^2\cos\varphi \tag{11}$$

Setting $\alpha = \frac{z_{load}}{Z}$, and substituting into Equation (9), one obtains:

$$F = 1 + \alpha^2 + 2\alpha\cos(\theta - \varphi) \tag{12}$$

To a certain extent, one can consider E, $\cos(\theta - \varphi)$, and Z unchanged, so that:

$$U = \frac{1}{\sqrt{F}}\frac{Z_{load}}{Z}E = \frac{\alpha}{\sqrt{F}}E \propto \alpha \tag{13}$$

$$I = \frac{1}{\sqrt{F}}\frac{E}{Z} \propto \frac{1}{1+\alpha} \tag{14}$$

After DG access into a load node, there is:

$$P'_{load} = P_{load} - P_{DG} = \lambda P_{load} \tag{15}$$

$$Q'_{load} = Q_{load} - Q_{DG} = \lambda Q_{load} \tag{16}$$

where λ is the proportion of the increase in node load, P_{load} and Q_{load} respectively equal the active and reactive power of the load, and P'_{load} and Q'_{load} respectively equal the active and reactive power of the load after increase. According to the Thevenin's theorem, the DG-containing distribution network is equivalent to the circuit shown in Figure 4, replacing Z_{load} with Z':

$$Z' = \frac{Z_{load}\cdot Z_{DG}}{Z_{load} + Z_{DG}} \tag{17}$$

After DG access, with $Z' < Z_{load}$.

When $Z' = Z$, the load-equivalent impedance and the line impedance are equal, and the line has the maximum transmission power. When Z' decreases, as $U \propto \alpha \propto Z'$ and $I \propto 1/\alpha \propto 1/Z'$, the corresponding current increases and the voltage decreases [23]. This is reflected in the PV curve; that is, the system runs on the upper part of the PV curve at normal operation, and the distance between the running point and the nose point represents the stability margin of the node voltage.

The conventional power flow equation is as follows:

$$\left.\begin{array}{l} P_i = V_i \sum\limits_{j \in i} V_j \left(G_{ij} \cos\theta_{ij} + B_{ij} \sin\theta_{ij}\right) \\ Q_i = V_i \sum\limits_{j \in i} V_j \left(G_{ij} \sin\theta_{ij} - B_{ij} \cos\theta_{ij}\right) \end{array}\right\} (i = 1, 2, \cdots, n) \tag{18}$$

Take Equation (17) as a continuous parameter equation, and combine with Equation (18), which is a normal power flow equation. By solving this equation set one can obtain the IVSE, and thus calculate the voltage stability margin. The PV curve can reflect the steady state behavior of the power system with load output changes. In order to obtain the IVSE and PV curves, the continuation power flow method is used to solve the above equations [24]. Equation (18) simplifies to a power flow equation with a parameter λ:

$$f(x, \lambda) = 0 \tag{19}$$

In this formula, $f \in R_n$, $x \in R_n$, $\lambda \in$ R, and the vector x contains the voltage magnitude and phase angle of all buses in the system. The value $\lambda = 0$ means there is no DG access. When λ takes another value, it represents the proportion of the increased load. Taking derivatives on both sides of Equation (19) yields:

$$df = \frac{\partial f}{\partial x} dx + \frac{\partial f}{\partial \lambda} d\lambda = 0 \tag{20}$$

Here dx denotes the change of system state due to the change of DG capacity, and $d\lambda$ denotes the change of equivalent load parameter due to the change of DG access position. By solving Equation (20) one obtains:

$$\begin{bmatrix} \widetilde{x}^{(i+1)} \\ \widetilde{\lambda}^{(i+1)} \end{bmatrix} = \begin{bmatrix} x^{(i)} \\ \lambda^{(i)} \end{bmatrix} + h \begin{bmatrix} dx \\ d\lambda \end{bmatrix} \tag{21}$$

In Equation (21), h is the step size; in order to make the estimated solution converge under the necessary constraints, set $h = 0.1$. Using the estimated solution produces the incremented solution $\widetilde{x}$. Then, for Equation (19), using an equation to augment the original power flow equation yields:

$$\begin{bmatrix} f(x, \lambda) \\ x_k - \widetilde{x}_k \end{bmatrix} = 0 \tag{22}$$

In Equation (22), x_k represents the continuation parameters, reflecting the voltage amplitude changes. By slightly modifying the conventional power flow process, one can solve Equation (22), and substitute the related parameters into Equations (1)–(6) to deduce the improved voltage stability evaluation index, the IVSE.

Through the derivation process of the IVSE index, one can infer the following characteristics. First, due to consideration of DG capacity changes, reducing the equivalent impedance and current at the access point thereby reduces network loss. Second, taking the change of voltage amplitude as an extension parameter, means the IVSE index can reflect the support of DG for the node voltage, and the distance between the IVSE index and one represents the voltage stability margin of this node. Third, by introducing parameter λ, which indicates the change of DG access position in the power flow equation, the index can reflect the power distribution of the system under different access nodes. The increased performance is reflected in the numerical value; that is, the IVSE value will be lower than the VSE, so that the network transmission capacity is improved.

Therefore, including the impact of DG, can, on the one hand, help reduce the loss of active power, and improve the nodes' stability so as to absorb more loads (that is, compared with the VSE, the IVSE will be reduced). On the other hand, it can reflect the impact on the system voltage profile and stability margin due to changes in the DG access location and capacity, which can be used to improve the system transmission capacity.

The solution of this model proceeds as follows: first, set the initial value of DG location and capacity, and initialize the related parameters. Then, determine the type and the load size of the connected nodes. Then, calculate the equivalent impedance of these nodes through Equations (17)–(22), and substitute into Equations (1)–(6) thus obtaining the IVSE value.

3. Simulation and Analysis

In this paper, our goal is to minimize the active loss. Adopting the variable load growth mode, with DG access in a centralized and decentralized method, the simulation is run with IEEE 33 & 69. The validity of the IVSE is verified by comparing the characteristic curves of VSE and IVSE.

Figure 5 shows the IEEE 33 & 69. The reference voltage is 12.66 kV, and the power reference value is 10 MVA [25]. The simulation is divided into two parts: one is the basic experiment without DG, the other is an experiment that includes DG access in different ways. Using a 33-node system, the total capacity of DG is set at 1.3 MW, with access into node 14 representing a centralized mode, and access into nodes 1, 5, and 14 representing a decentralized mode [26,27]. The capacity is increased by 10%, 30%, 50%, 60%, 80%, and 100% increments. Next, in a 69-node system, centralized DG access is into node 50, and decentralized access [28] is into nodes 11, 18, and 50.

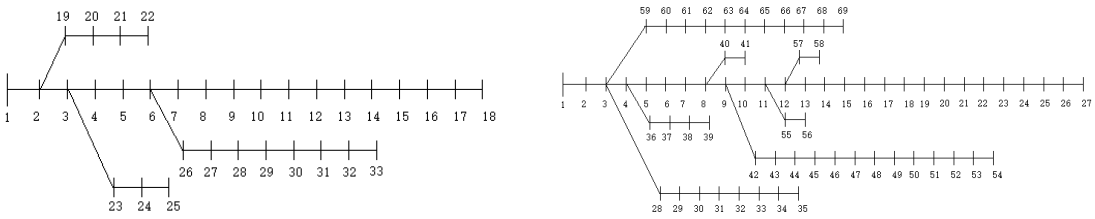

(**a**) IEEE 33 (**b**) IEEE 69

Figure 5. IEEE 33 & 69 distribution system diagram.

3.1. Simulations

With the initial load condition and without DG, the VSE calculation results of each node in the 33-node system are shown in Figure 6. From Figure 6a, we can see that the VSE of node 5 is the largest, and that the voltage stability margin of this node is the lowest, so the voltage stability of this node is the weakest. When load increases, this node may incur voltage collapse first.

When adopting variable load growth mode (that is, all the nodes in the net increase or decrease in different proportions from the initial load level), we take 0.1 MW as a step, and do increments with the same ratio, up to the voltage collapse point. The results are shown in Figure 6b.

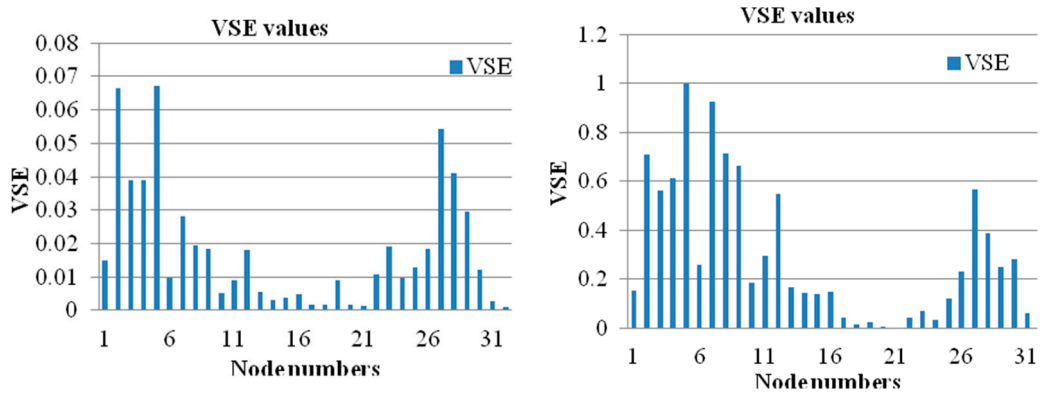

(**a**) initial conditions (**b**) critical conditions

Figure 6. VSE index values under different conditions (Node 33).

From Figure 6b we can see that, when the voltage is near the collapse point, the node 5 VSE increases to one first. To verify this conclusion, we consider some relevant PV curves. Select node 5 with the biggest VSE, node 18 with the smallest VSE, and node 9 in the middle.

The corresponding PV curves are shown in Figure 7a. In Figure 6b, the ordinate represents the voltage amplitude (pu.), while the abscissa represents the active power (kVA). The same method is used for the 69-node system, and the results are shown in Figure 7b. From the simulation results, for the 33-node system, when the system reaches the critical point of voltage stability, the limit power is about 1.31 MW. The critical voltage of node 5 is 0.673 (pu., for this and the following values), that of node 9 is 0.583 and that of node 18 is 0.5303; that is, the voltage stability margin of node 5 is 0.327, node 9 is 0.417, and node 18 is 0.4697.

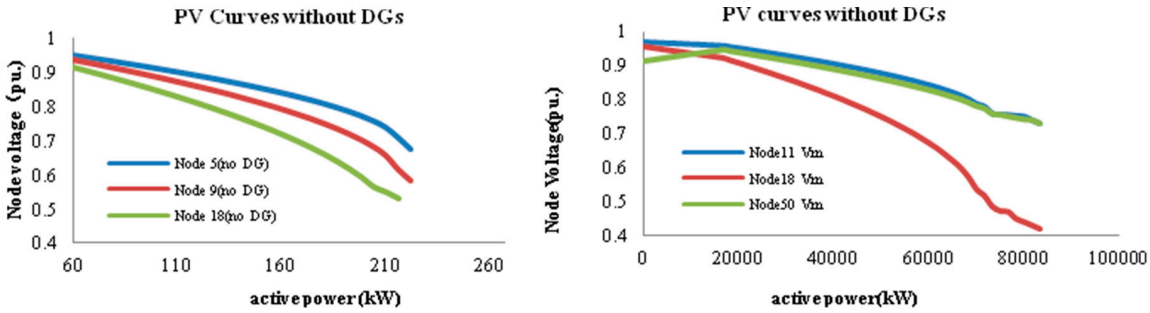

(**a**) IEEE 33 (**b**) IEEE 69

Figure 7. PV curves without DG during load increasing process.

In the 69-node system, when the system reaches the critical point of voltage stability, the limit power is about 5 MW, the critical voltage of node 11 is 0.74, that of node 18 is 0.49 and that of node 50 is 0.73; that is, the voltage stability margin of node 11 is 0.26, node 18 is 0.51, and node 50 is 0.27.

When the influence of DG is considered in the power flow calculation and the IVSE index is used as the judgment condition when the system voltage approaches the collapse point, according to the above analysis, the voltage stability level and the transmission power limit of the system will be improved. Figure 8 shows the curves of the nodes 5, 9, and 18 and the nodes 11, 18, and 50 in the 33-node and 69-node system, respectively, as the load increases to the critical point of the voltage collapse. From these curves, we see that the ability of the system to transmit at maximum power is improved. This improvement in maximum transmitted power would not be reflected in the VSE, but requires the IVSE to be fully observed.

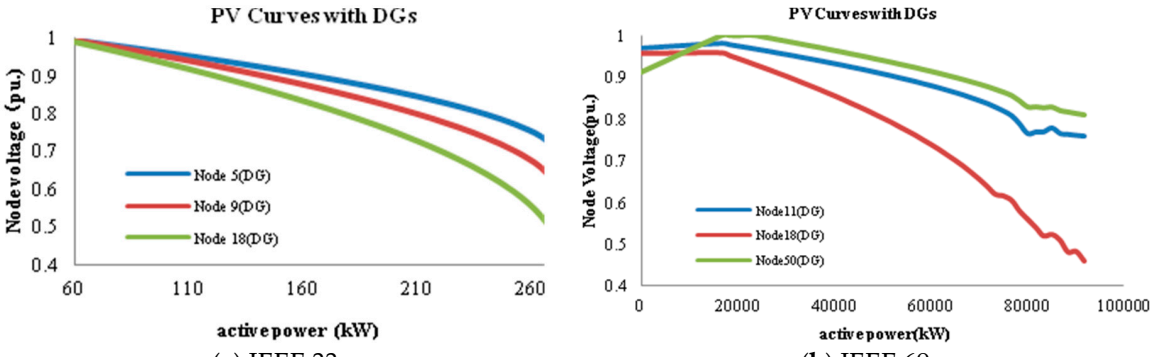

(**a**) IEEE 33 (**b**) IEEE 69

Figure 8. PV curves with DG during load increasing process.

3.2. Centralized and Decentralized Access

3.2.1. Centralized Access

For the 33-node and 69-node system, the weakest nodes, node 5 and node 14, are taken as example points, using the configuration above. The study below mainly focuses on the change of the maximum power, net loss and IVSE after including DG access. The results are shown in Table 1.

Table 1. Limit power and network loss in centralized access mode with DG (Node 33 & 69).

DG Access Centralized						
After DG Access			**Initial Load Condition (Unit: MW)**			
DG Access Ratio	**Limit Power**		**Active Power Loss**		**Reactive Power Loss**	
	33-Node	**69-Node**	**33-Node**	**69-Node**	**33-Node**	**69-Node**
0%	1.31	0.5	0.202	0.226	0.134	0.102
10%	1.308	0.5	0.186	0.197	0.122	0.089
30%	1.308	0.51	0.159	0.149	0.105	0.068
50%	1.308	0.51	0.142	0.115	0.092	0.053
60%	1.296	0.51	0.135	0.103	0.088	0.047
80%	1.296	0.51	0.128	0.087	0.081	0.04
100%	1.296	0.52	0.128	0.081	0.077	0.036

From the simulation results, we can see that, for the 33-node system, with the increase in DG output, the system's maximum power has nearly no change, but the net loss decreases; meanwhile, for the 69-node system, the limit power increases and the net loss decreases. In order to derive the IVSE index, as mentioned above, the change of DG access capacity is included in the power flow calculation. The simulation results show that with the increased DG capacity, network loss is reduced and transmission capacity is increased.

The node voltage profile curves are shown in Figure 9a,b, respectively, for the 33-node and 69-node systems. This shows that when the DG is connected to one centralized point, with the increase of DG access capacity, the voltage at the access point and its nearby nodes changes greatly, but there is little effect on the overall voltage profile of the network. Similarly, in deriving the IVSE, and for obtaining the PV curves, an increment of the node voltage amplitude is introduced into the power flow calculation. The simulation results show that the DG has a significant supporting effect on the voltage at the access point.

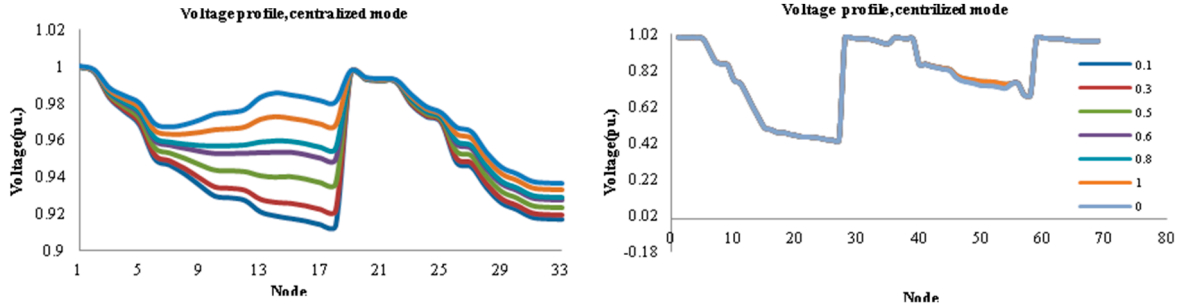

(**a**) IEEE 33 (**b**) IEEE 69

Figure 9. Voltage profile of all nodes in net under centralized mode with DG.

Figure 10 shows how the voltage stability index calculated from node 5 (33-node) and node 14 (69-node) increases when the load changes, with DG access in a centralized mode with different outputs: (1) there is no DG, that is, the output is 0; (2) DG output 60%; (3) DG output 100%.

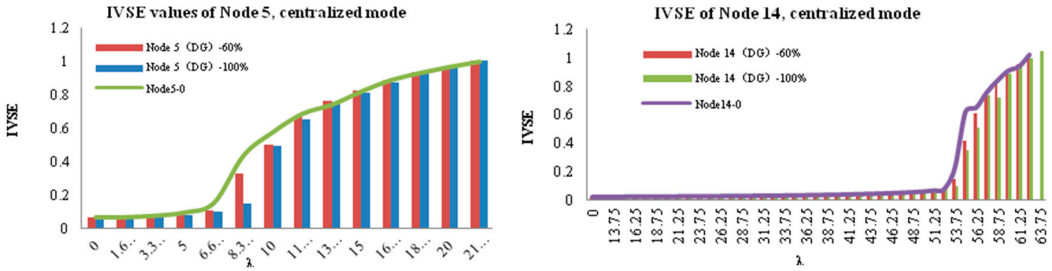

(**a**) IEEE 33 (**b**) IEEE 69

Figure 10. The IVSE index in centralized access mode.

For the 33-node system, in the initial state, when the voltage stability index of node 5 reaches 1, the value of λ is 21.67; in the case of the rated output of the DG, when the index of node 5 reaches 1, the value of λ increases to 23.3. For the 69-node system, when node 14 reaches 1, in the initial state, λ is 62.5; in the rated output state, λ increases to 63.7. These results indicate that the inclusion of DG can help improve the ability of the node in the net to accept more loads. When the IVSE index approaches one, it indicates that the system approaches the stability limit, and λ indicates the proportion of load increase. The higher the proportion, the greater the load capacity the node can access when the stable limit point is reached. The simulation results show that using the IVSE index as a criterion can reflect the increased access capacity due to DG.

The curve in Figure 10 shows the index value without DG, and the histogram represents the change of IVSE when DG output is 60% and 100%. With the increase of DG output, the IVSE value decreases and the node voltage stability margin increases. This shows that the IVSE index can reflect the impact on the system due to the change of DG capacity.

The above analysis shows that using the IVSE as an evaluation index, under the centralized access mode, helps to improve the voltage of the access point and its nearby nodes, and reduces network loss but has little effect on the overall system voltage profile. Meanwhile, because the variation of DG capacity is considered in the derivation process of IVSE, compared with the VSE, it can better reflect the influence of DG capacity change on system power flow distribution.

3.2.2. Decentralized Access

For the 33-node and 69-node system, DG access occurs at nodes 5, 9, and 18 and nodes 11, 18, and 50, respectively. Using nodes 5 and 14 as examples, we analyze the system limit power, net loss and voltage profile, and the VSE and IVSE changes.

As shown in Table 2, for the 33-node and 69-node systems, with the increase in DG output, the limit power of the system is increased and the network loss is reduced. Compared with the findings in Table 1, when DGs access with the same capacity, the decentralized access mode is better than the centralized mode in improving the limit power and reducing network loss.

Table 2. Limit power and network loss in decentralized access mode with DG (Node 33 & 69).

DG Access Decentralized						
After DG Access			Initial Load Condition (Unit: MW)			
DG Access Ratio	Limit Power		Active Power Loss		Reactive Power Loss	
	33-Node	69-Node	33-Node	69-Node	33-Node	69-Node
0%	1.31	0.5	0.202	0.226	0.134	0.102
10%	1.332	0.51	0.182	0.194	0.122	0.088
30%	1.368	0.52	0.165	0.142	0.11	0.064
50%	1.38	0.53	0.149	0.105	0.098	0.048
60%	1.404	0.53	0.139	0.091	0.091	0.042
80%	1.464	0.54	0.131	0.074	0.084	0.034
100%	1.5	0.55	0.122	0.068	0.078	0.031

For the 33-node and 69-node systems with the decentralized access mode, the voltage profile curves are shown in Figure 11a,b, respectively. Comparing with the centralized mode, not only the access point voltage but also the voltage profile of the whole system are improved, and the amplitude is balanced.

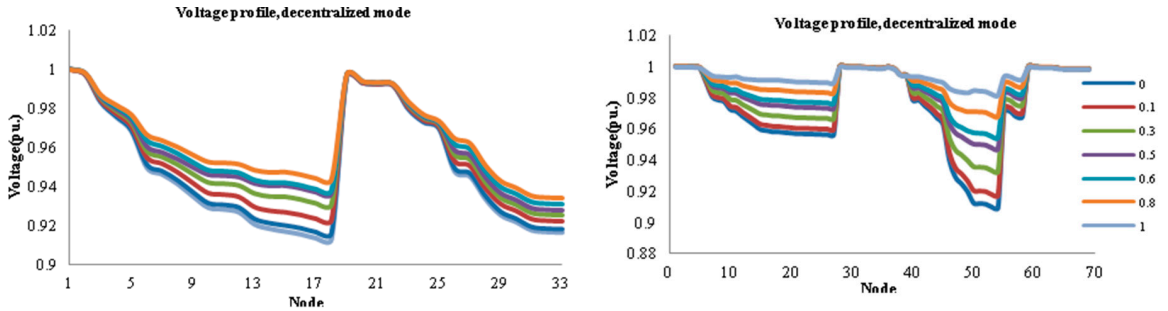

(**a**) IEEE 33 (**b**) IEEE 69

Figure 11. Voltage profile of all nodes in net under decentralized mode with DG.

When the DG output adopts the same three magnitudes (0, 60%, 100%) as described above. The result is the IVSE and VSE curves that are shown in Figure 12.

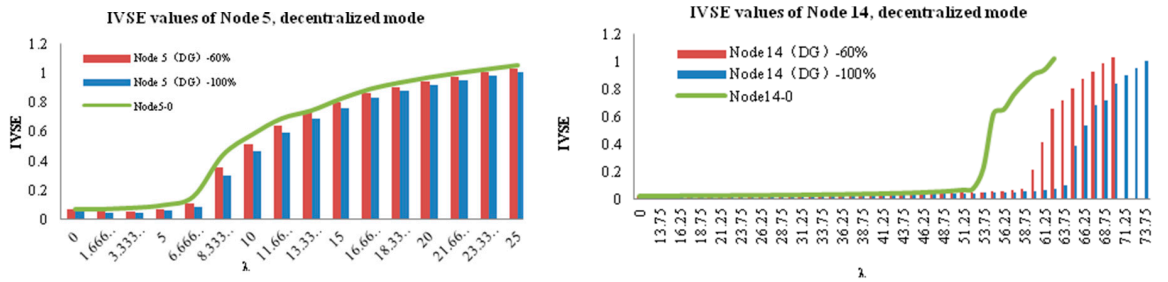

(**a**) IEEE 33 (**b**) IEEE 69

Figure 12. Voltage profile of all nodes in net under decentralized mode with DG.

Figure 12 demonstrates that for the 33-node and 69-node systems, with DG access in decentralized mode, as the IVSE value decreases, the node voltage stability margin increases; that is, the ability to accept the load improves. The simulation results show that, for the 33-node system, when the IVSE index of node 5 reaches 1, the value of λ increases to 25. For the 69-node system, in the same state, when node 14 reaches 1, the value of λ increases to 68.75. Compared with the case of no DG access and centralized access, in the decentralized mode, the value of λ increases more, meaning that the system can accept a larger capacity of DG. Therefore, the IVSE can also reflect the change of DG capacity on the power flow distribution under different access modes.

Figure 13 compares the IVSE and VSE, under different access capacities and location modes. Node 5–60% (100%) represents the VSE value in the state of DG output is 60% (100%); Node 5 (DG)–60% (100%) represents the same state of the IVSE index.

As Figure 13 demonstrates, the trend for IVSE and VSE are basically the same, but with the increase of DG access capacity, the VSE index remains unchanged, while the IVSE index decreases and is lower than the VSE. This shows that both of the above two indexes suffice as evaluation indexes in judging whether the system reaches the stability limit and reflecting the capability of the system to accept DGs. However, compared with the traditional VSE index, the IVSE index can better reflect the influence on system power flow of changes in DG access capacity and location. Thus, the IVSE can be used as an evaluation index of system voltage stability accounting for DG access.

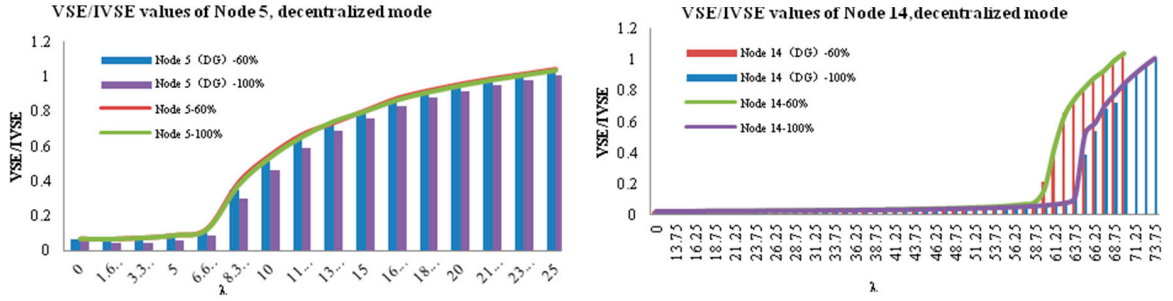

(**a**) IEEE 33 (**b**) IEEE 69

Figure 13. The VSE/IVSE index of node 5 in decentralized access mode.

4. Comparison of Results

Tables 3 and 4 present the produced results as well as the results of traditional methods that have been applied and tested on both the IEEE 33 & 69 distribution system and have been presented in References [29,30]. The results obtained with the proposed method are comparable to those produced by the traditional methods, something which clearly implies that the proposed method works well and has an acceptable accuracy.

Table 3. Comparison of results for 33-node distribution network.

References	Methods Used	Access Mode	Size of DG/DGs (MW)	Active Loss (MW)
Ref. [29]	Analytical method	centralized	2.5	0.1112
Ref. [30]	GA PSO	decentralized	1.5/0.423/1.0714 1.177/0.982/0.83	0.1063 0.1053
Proposed method	Evaluation method	centralized decentralized	2.8 0.754/1.099/1.071	0.1054 0.101

Table 4. Comparison of results for 69-node distribution network.

References	Methods Used	Access Mode	Size of DG/DGs (MW)	Active Loss (MW)
Ref. [29]	Analytical method	centralized	1.8078	0.0834
Ref. [30]	GA PSO	decentralized	0.9297/1.0752/0.985 0.993/1.1998/0.796	0.089 0.0832
Proposed method	Evaluation method	centralized decentralized	1.873 0.6267/0.5805/1.719	0.0839 0.0699

5. Discussion

The produced results show that high penetration access of DGs has a significant impact on the voltage profile and power loss of the distribution network. DG access has a positive effect on reducing the power loss of the distribution network, and generally this decrease is proportional to the DGs capacity. On the other hand, with DG access of different locations, the voltage profile of the distribution network can be improved to a different extent. Generally, when DGs access a relatively weak node in the net, it can improve the voltage support for the access node and its surrounding nodes, so to improve the local voltage profile. In addition, DG different access mode has a crucial impact on the voltage profile and net loss of the whole distribution network. Through the simulation above, it can be observed, normally, that when DGs take a decentralized mode, it can better improve the voltage profile and reduce net loss.

Furthermore, through the experiments described above, compared with the traditional VSE index, the IVSE can more effectively reflect the influence of DG access position and capacity change on

the power transmission limit and the ability of the distribution network to receive the DG. At the same time, IVSE index has the characteristics of being easy to understand, having simple calculation, and having a flexible setting of parameters. Therefore, the IVSE index proposed in this paper can be used as a reference evaluation index for DG optimization.

The proposed evaluation method results, produced for the IEEE 33 & 69 node system, have been compared with results obtained from a previous method for the same distribution system. The comparison has shown that the proposed method is efficient and can provide a good solution for the optimum position and capacity of DG in distribution network.

Thus far, types of DG technologies in this country are developing rapidly. However, the original distribution network did not consider the high penetration of DG in the initial planning. The result is a serious phenomenon of abandonment of wind and solar power, which has a worse impact on the stability, power quality and other aspects of the distribution network. In order to solve such problems, it is necessary to propose a universal, simple and practical evaluation system, which can provide a basis for distribution network planners to refer to. This is particularly essential during the process of distribution network planning or reconstruction, so the impact of DG access can be taken into account seriously to improve the ability and level of the distribution network to accept various new energy sources. Such problems also exist in the technique by which electric vehicles are connected to the distribution network. As a further work, the access problem of electric vehicles will be studied and taken into account, targeting the further development of the proposed method, and will also be applied to studies of an existent distribution network.

6. Conclusions

In this paper, a static stability model was presented. This model corrects the conventional power flow equations by accounting for the characteristics of DG, and is simple, easy to understand, and versatile. Through solving this model mathematically, we obtain the IVSE index, which can reflect the high penetration of DG. Simulations with 33-node and 69-node systems were performed, the results of which verified the effectiveness of the IVSE index. The simulations showed that, when DGs access their net in the proper location and capacity, one can optimize the power flow distribution, reduce the network loss, improve the transmission capacity of the system, and enhance the stability of each node voltage. This is particularly true when the DG adopts the decentralized access mode. The IVSE index shows the influence of DGs on the system voltage profile, network loss, and maximum power more accurately than the VSE, changing to reflect DG location and capacity. The IVSE index is very suitable for research on site selection for distributed generation.

Acknowledgments: Fund project: National Key Research and Development Program of China under Grant Number 2016YFB0101900.

Author Contributions: Jingjing Tu and Zhongdong Yin conceived and designed the experiments; Jingjing Tu performed the experiments; Jingjing Tu analyzed the data; Haiyong Xu contributed analysis tools; Jingjing Tu wrote the paper.

Conflicts of Interest: The authors declare no conflict of interest.

References

1. Shu, Y.; Zhang, Z.; Guo, J.; Zhang, Z. Study on Key Factors and Solution of Renewable Energy Accommodation. *Proc. CSEE* **2017**, *37*, 1–8.
2. Ackerman, T.; Anderson, G.; Seder, L. Distributed generation: A definition. *Electr. Power Syst. Res.* **2001**, *57*, 195–204. [CrossRef]
3. Ma, Z.; An, T.; Shang, Y. State of the Art and Development Trends of Power Distribution Technologies. *Proc. CSEE* **2015**, *36*, 1552–1567.
4. Chen, G.; Li, M.; Xu, T.; Liu, M. Study on Technical Bottleneck of New Energy Development. *Proc. CSEE* **2017**, *37*, 20–26.

5. Lin, S.; Li, X.; Liu, Y. Present Investigation of Voltage Stability and Composite Load's Influence on It. *Proc. CSU-EPSA* **2008**, *20*, 66–74.
6. Zhong, W.; Tang, Y. Transient Voltage Stability Analysis of Differential-algebra Equation in Power System. *Proc. CSEE* **2010**, *30*, 10–16.
7. Chen, N.; Zhu, L.; Wang, W. Strategy for Reactive Power Control of Wind Farm for Improving Voltage Stability in Wind Power Integrated Region. *Proc. CSEE* **2009**, *29*, 102–108.
8. Chen, Q.; Li, L.; Wang, Q.; Zeng, Y. Simulation Model of Photovoltaic Generation Grid-Connected System and Its Impacts on Voltage Stability in Distribution Grid. *Trans. China Electr. Tech. Soc.* **2013**, *28*, 241–247.
9. Liu, X.-D.; Guo, R.; Zhang, J.-F.; Zeng, R.-M. Voltage stability assessment frame for distribution network with wind farms. *Power Syst. Prot. Control* **2013**, *41*, 77–81.
10. Qin, W.; Ren, C.; Han, X.; Wang, P.; Liu, Z. Power System Voltage Stability Risk Assessment Considering the Limit of Load Fluctuation. *Proc. CSEE* **2015**, *35*, 4102–4111.
11. Bai, Y.; Wang, P.; Han, X.; Qin, W. Risk Assessment of Static Voltage Stability Based on Load Uncertainty Modeling. *Proc. CSEE* **2016**, *36*, 3470–3478.
12. Vita, V. Development of a decision-making algorithm for the optimum size and placement of distributed generation units in distribution networks. *Energies* **2017**, *10*, 1433. [CrossRef]
13. Vita, V.; Alimardan, T.; Ekonomou, L. The impact of distributed generation in the distribution networks' voltage profile and energy losses. In Proceedings of the 9th IEEE European Modeling Symposium on Mathematical Modeling and Computer Simulation, Madrid, Spain, 6–8 October 2015; pp. 260–265.
14. Zhang, Y.; Zhou, S.; Wang, L.; Huang, Y.; Zhang, G. The Theoretical Foundations of Static Voltage Stability Analysis Model. *Proc. CSEE* **1999**, *19*, 55–63.
15. Paramasivam, M.; Salloum, A.; Ajjarapu, V.; Vittal, V.; Bhatt, B.; Liu, N. Dynamic optimization based reactive power planning to mitigate slow voltage recovery and short term voltage instability. *IEEE Trans Power Syst.* **2013**, *28*, 3865–3873. [CrossRef]
16. Amrane, Y.; Boudour, M.; Belazzoug, M. A new optimal reactive power planning based on differential search algorithm. *Int. J. Electr. Power Energy Syst.* **2015**, *64*, 551–561. [CrossRef]
17. Lu, Z.; Li, H.; Qiao, Y. Flexibility Evaluation and Supply/Demand Balance Principle of Power System with High-penetration Renewable Electricity. *Proc. CSEE* **2017**, *37*, 9–19.
18. Jiang, T.; Ai, L.; Yang, Y. On-ling voltage stability index based on load margin. *Electr. Power Autom. Equip.* **2009**, *29*, 39–42.
19. Sheng, W.; Liu, K.Y.; Liu, Y.; Meng, X.; Li, Y. Optimal placement and sizing of distributed generation via an improved non-dominated sorting genetic algorithm II. *IEEE Trans. Power Deliv.* **2015**, *30*, 569–578. [CrossRef]
20. Zeinalzadeh, A.; Mohammadi, Y.; Morad, M.H. Optimal multi objective placement and sizing of multiple DGs and shunt capacitor banks simultaneously considering load uncertainty via MOPSO approach. *Int. J. Electr. Power Energy Syst.* **2015**, *67*, 336–349. [CrossRef]
21. Tan, Y.; Li, X.; Cai, Y.; Wang, C. Modeling Cascading Failures in Power Grid Based on Dynamic Power Flow and Vulnerable Line Identification. *Proc. CSEE* **2015**, *35*, 615–622.
22. Zheng, Y.; Sun, J.W.; Zhang, C.; Lin, X.N. Study of Voltage Stability Margin for the Distribution Network with Electric Vehicle Integration. *Trans. China Electr. Tech. Soc.* **2014**, *29*, 20–26.
23. Prabha, K. *Power System Stability and Control*; McGraw-Hill Education: New York, NY, UAS, 1994.
24. Wang, X. Modern Power System Analysis. *Sci. Press* **2003**, *1*, 66–68.
25. He, J.; Chen, G.Y.; Tao, Z.D.; Wang, Y.J.; Xu, G.J. Reactive Power Optimization in Distribution System with Distributed Generators Considering Voltage Stability Index. *Shanxi Electr. Power* **2015**, *43*, 30–31.
26. Hu, H.; Wu, S.; Xia, X.; Gan, D. Computing the Maximum Penetration Level of Multiple Distributed Generators in Distribution Network Taking into Account Voltage Regulation Constraints. *Proc. CSEE* **2006**, *26*, 13–19.
27. Kim, T.E.; Kim, J.E. Considerations for the feasible operating range of distributed generation interconnected to power distribution system. In Proceedings of the IEEE PES Summer Meeting, Chicago, IL, USA, 21–25 July 2002.
28. Hung, D.Q.; Mithulananthan, N.; Lee, K.Y. Optimal placement of dispatchable and nondispatchable renewable DG units in distribution networks for minimizing energy loss. *Electr. Power Energy Syst.* **2014**, *55*, 179–186. [CrossRef]

29. Gozel, T.; Hocaoglu, M.H. An analytical method for the sizing and sitting of distributed generators in radial systems. *Electr. Power Syst. Res.* **2009**, *79*, 912–918. [CrossRef]
30. Moradi, M.H.; Tousi, S.M.R.; Abedini, M. Multi-objective PFDE algorithm for solving the optimal sitting and sizing problem of multiple DG sources. *Int. J. Electr. Power Energy Syst.* **2014**, *56*, 117–126. [CrossRef]